A compact molecular beam machine

Jansen, P.; Chandler, D.W.; Strecker, K.E.

published in
Review of Scientific Instruments
2009

DOI (link to publisher)
10.1063/1.3206367

document version
Publisher's PDF, also known as Version of record

A compact molecular beam machine

Paul Jansen,[1] David W. Chandler,[2] and Kevin E. Strecker[2,a)]
[1]*Vrije Universiteit, 1081 HV Amsterdam, The Netherlands*
[2]*Sandia National Laboratories, Livermore, California 94551, USA*

(Received 8 May 2009; accepted 27 July 2009; published online 31 August 2009)

We have developed a compact, low cost, modular, crossed molecular beam machine. The new apparatus utilizes several technological advancements in molecular beams valves, ion detection, and vacuum pumping to reduce the size, cost, and complexity of a molecular beam apparatus. We apply these simplifications to construct a linear molecular beam machine as well as a crossed-atomic and molecular beam machine. The new apparatus measures almost 50 cm in length, with a total laboratory footprint less than 0.25 m^2 for the crossed-atomic and molecular beam machine. We demonstrate the performance of the apparatus by measuring the rotational temperature of nitric oxide from three common molecular beam valves and by observing collisional energy transfer in nitric oxide from a collision with argon. © *2009 American Institute of Physics.*
[DOI: 10.1063/1.3206367]

I. INTRODUCTION

Atomic and molecular beams (AMBs) have been used for nearly a century to isolate and study the properties and behavior of atoms and molecules, which has led to several monumental advances in scientific understanding. The first beam experiments were in 1919 by Stern[1] in which he used atomic silver beams to test the Maxwell–Boltzmann velocity distribution. In 1922, Stern and Gerlach[2] performed their famous experiment demonstrating that atoms have intrinsic spin and that the spin is quantized. Then in the 1930s Rabi and Cohen[3] demonstrated the effects of the nuclear magnetic moment in atomic beams. By the 1960s, Wilson *et al.*[4] crossed two atomic beams to study collisions of alkali atoms and later to observe reactions between atoms and molecules from a single collision. Herschbach[5] was then joined by Lee, who developed techniques to extract detailed angular distributions for scattered products using an ionizing filament and a rotatable detector. With his "universal detector," Lee was able to determine the angle and the kinetic energy of collision products. The 1986 Nobel Prize in chemistry was awarded to Herschbach, Lee, and Polanyi "for their contributions concerning the dynamics of chemical elementary processes."[6]

By the late 1970s, advances in laser technology led to the ability to perform state specific ionization using resonance enhanced multiphoton ionization (REMPI).[7] REMPI allowed for quantum state specific total cross sections to be collected. In the late 1980s, Houston and Chandler[8] developed the ion-imaging technique which uses REMPI to get quantum state specific information, and a set of ion optics and microchannel plate coupled to a phosphor screen to get spatial information. Suits *et al.*[9] demonstrated the application of the ion-imaging technique to crossed-AMB (CAMB) scattering in 1992. This process allowed recovery of the entire differential cross section of the ionized products of a collision for all angles in a single image.

The fundamentals of molecular beam technology and experiments have been detailed in Ref. 10, which covers the design and construction of molecular beam experiments, and Ref. 11, which discusses novel experimental techniques. For the discussion here, we will primarily focus on the design of the CAMB machines discussed in these books: note a linear machine is simply half of a CAMB machine.

CAMB machines typically consist of a large primary chamber impregnated with two source regions and either a movable time-of-fight mass spectrometer or an ion-imaging system. The chambers are relatively large to accommodate large diffusion pumps or turbo-molecular pumps needed to remove the large amounts of gas injected into the source regions from the molecular beam nozzles, which is traditionally a continuous flow valve. The source chambers are built inside the main chamber housing the scattering region in order to minimize the distance from the nozzle to the interaction region, thus maximizing the density of particles at the interaction region. In order to obtain well-collimated, velocity-selected beams, the source is usually differentially pumped, making the typical apparatus several meters in length, and costing hundreds of thousands of dollars to construct.

The pumping and background pressures (signal-to-noise) for these apparatuses are typically estimated by constructing a Thevenin-type diagram for the vacuum system. This analysis treats the vacuum components as electrical components. The valve is treated as a current source, conduction limiters as resistors, chambers as capacitors, and pumps as current sinks. In order to achieve the high pumping speed, using common components, the use of large nonconduction limited pumps is required. This, combined with the detection schemes and minimizing the distance from the nozzle to the

a)Electronic mail: kstreck@sandia.gov.

source, leads to the use of large vacuum chambers with large (and expensive) diffusion or turbo-molecular pumps.

In this article, we demonstrate that by combining recent advances in molecular beam technology with modern advances in ultrahigh vacuum (UHV) pumping technology, we are able to construct a very small modular molecular beam machine. This new apparatus is capable of either unimolecular or bimolecular beam studies. This new compact CAMB (C-CAMB) machine costs a fraction of the price of a traditional apparatus, largely due to the decreased size of the vacuum chambers and the UHV pump sizes required. The C-CAMB machine measures approximately 50 cm in length, with a laboratory footprint less then 0.25 m^2.

II. DISCUSSION

There are two major technological advancements over the past few decades that have enabled us to reanalyze the operation of AMB machines: the pulsed molecular beam valve,[10] and advancements in turbo-molecular pumping. When these two technologies are taken together with the ion-imaging detection scheme, we are able to reduce the size and complexity of the AMB machine itself, which greatly reduces construction costs.

Several types of pulsed molecular beam valves have been developed. The most common valves employed are the solenoid actuated (General) valve,[12] and the piezoelectric (PZT) actuated (Trickl) valve.[13] Both valve types have pulses on the time scale of a few hundred microseconds. More recently, bimetal (Jordan) valve[14] and magnetic amplified solenoid [Even–Lavigne (EL)] valve[15] have been developed. These valves have minimum pulse lengths in the tens of microseconds. The short pulses, hundreds of microseconds or less, reduce the overall gas load into the vacuum system, allowing for dense beams, while reducing the pumping requirements.

To determine the pumping required, one needs to understand how the gas, once injected into the system, is pumped out of the system, and what background gas levels are acceptable for the desired experiment. For this new apparatus, instead of using the Thevenin treatment to calculate the steady state gas load on the system, we simulated the time-dependent behavior of an ideal gas in the vacuum system. For the sample system, we chose a cubic chamber with no internal structure and a pump located at one wall of the cube.

We simplified the calculations by noting that there are two distinct regions in vacuum technology of interest; viscous flow and molecular flow. The regions are defined by the relationship between the mean free path of the molecules, and the size of the vacuum chamber. At pressures where the mean free path is very short compared to the distance between chamber walls, particles predominantly have collisions with each other. Rapid momentum transfer happens from particle to particle, resulting in a viscous flow of particles. At low pressures, where the mean free path is long compared to the dimensions of the vacuum chamber, the particles primarily exchange momentum with the walls. As a result, the particle motion is statistical, which is the molecular flow regime. In this molecular flow regime, particles must find the pumps through diffusion. The pumping dynamics of an ideal gas in the test chamber depend on the steady-state background pressure and the dimensions of the source chamber (mean free path compared with the chamber size); if the pressure is high enough, the pumping dynamics will be governed by viscous flow, and at lower pressures molecular flow will dominate.

The primary design concern is the ability for the source region to maintain steady-state pressure low enough as not to quench the supersonic expansion and to produce a molecular beam that is internally (rotationally and vibrationally) cold. The important length scale for the mean free path is taken to be the distance between the gas valve and beam skimmer. This distance is typically a few centimeters or less to ensure a high density of particles in the beam, and to reduce choking of the supersonic expansion from the background gas. With this assumption for the valve to skimmer distance, operating at a typical steady state pressure of 1×10^{-3} Torr, the pumping dynamics of the source region are dominated by molecular flow.

The mean free path for a thermal gas l is given by

$$l = \frac{1}{\sqrt{2}} \frac{RT}{\pi d^2 N_A P}, \tag{1}$$

where R is the ideal gas constant, T is the temperature, d is the hard sphere diameter of a gas molecule, N_A is the Avogadro constant, and P is the pressure. A typical room temperature gas has a hard sphere diameter of $\sim 3.5 \times 10^{-10}$ m. A maximum source chamber pressure is 1×10^{-3} Torr, is chosen as an upper limit for this discussion because we experimentally observe choking of the supersonic expansion near this pressure in our traditional CAMB experiments. Using these parameters, we calculate a mean free path of 5.7 cm, which is longer than the nozzle to skimmer distance.

Treating the molecular motion in the chamber by diffusion allows us to construct a simple model for the pumping of the chamber. In the molecular flow regime, the pumps do not pump; thus, we treat pumps as "sticky walls." The molecule must diffuse into a vacuum pump, where it has a probability of "sticking." The rate at which gas is removed from the system is determined by the probability of a particle finding the pump, and a weighted sticking factor, rather than the specified pumping speed of the pump. The sticking factor is an approximation to account for issues such as pump design, rotation speed, and backstreaming of light particles.

This simplistic model suggests that the primary criteria governing the pumping dynamics of the vacuum chamber is the ratio of the internal area of the chamber walls to the total pump opening area. The pumping speed is determined by the probability for a particle to find a pump through random diffusion. To optimize the pumping for the source region, we want to minimize the internal area of the source chamber, while maximizing the pumping area. To achieve this, we use recently available turbo-molecular pumps on ISO-KF 40 and CF2.75 flanges (available from nearly all pump manufacturers). The small size of these pumps allows for nearly an entire wall of a CF2.75 cube to be a pump, maximizing the ratio of the pumping area to the internal area of the chamber.

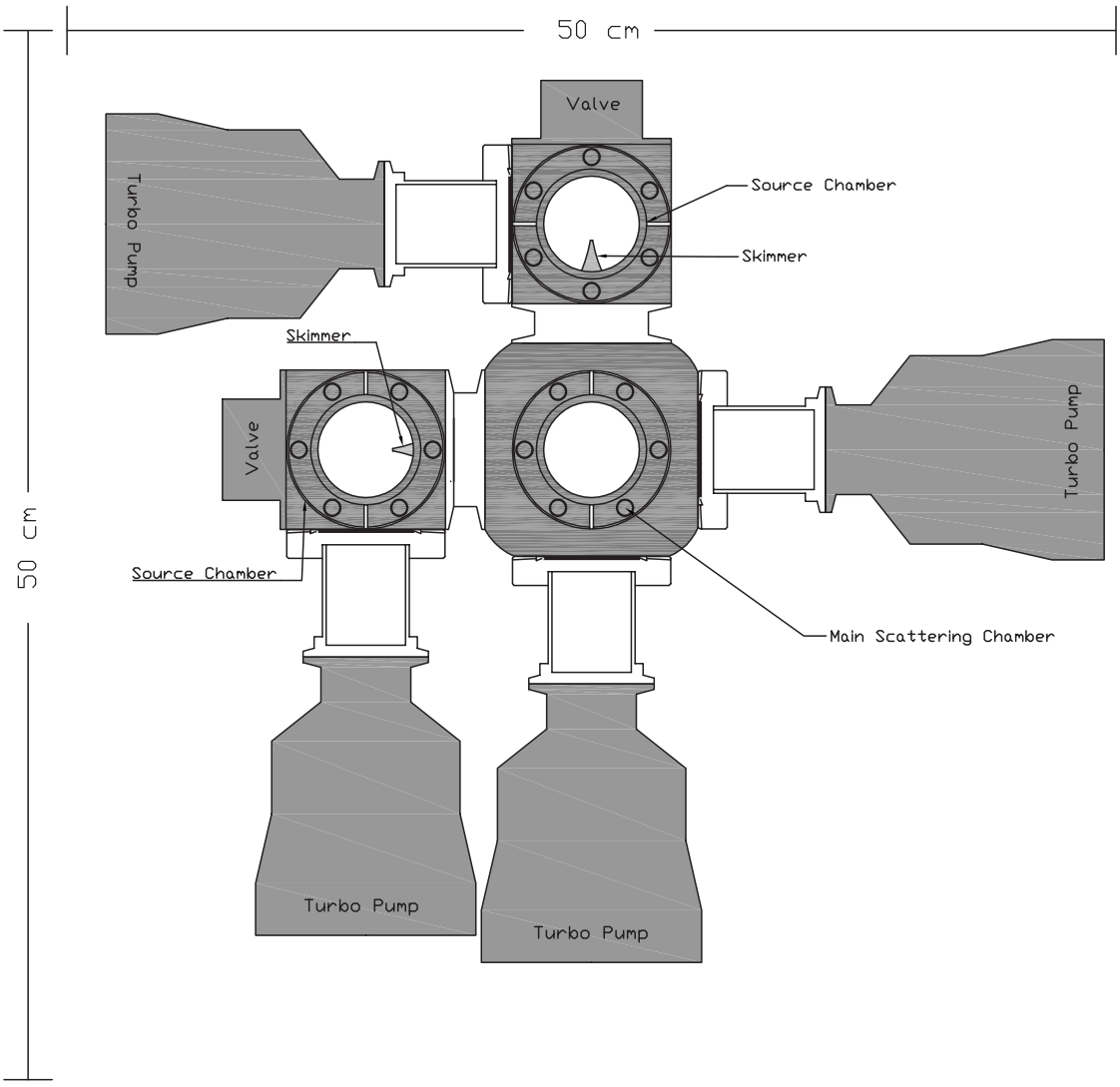

FIG. 1. Schematic diagram of the C-CAMB. The major components are shown with the correct relative scale. Other components, such as gauges, vent valves, and roughing forelines are not shown for improved clarity.

Using these components, we constructed a C-CAMB machine (see Fig. 1) using standard CF2.75 parts, reducing the size and cost of the apparatus without sacrificing performance.

III. THE APPARATUS

Figure 1 shows a schematic depiction of our C-CAMB machine. The unimolecular machine is constructed by removing one arm of the C-CAMB machine. The C-CAMB apparatus consists of two source regions, a main or interaction chamber, and four turbo-molecular pumps. The source regions are separated from the main chamber by Beam Dynamics skimmers with approximately 0.7mm orifices. The distance between the valve face and the skimmer is 4.4 cm.

Each source chamber is constructed from a single CF2.75 Kimball Physics spherical cube, model MCF275-SC600. The source chambers are each pumped by a single hybrid turbo molecular pump, Adixen ATH 31+mounted on an ISO-KF 40 flange. The main chamber consists of a single Kimball Physics extended spherical cube, model MCF275-ESC608. The main chamber is pumped by either one or two of the Adixen hybrid turbo molecular pumps, depending on the experimental configuration. The source regions are attached to the main chamber at 90° to each other. All four hybrid turbo molecular pumps are rough pumped by a single Pfiffer OnTool Dry-pump, model PTK16919, specified for pumping corrosive media. The roughing pump has a maximum pumping speed of 84 m^3/h with an ultimate pressure $<3.7\times10^{-2}$ Torr.

To characterize the operation of the system we used two detection methods; laser-induced fluorescence (LIF) and velocity-mapped ion-imaging (VMII). Each scheme requires a different pump arrangement and a different setup on the vertical axis of the main chamber. The LIF setup uses two hybrid turbo molecular pumps collinear with each source region as depicted in Fig. 1. A $f=25$ mm planoconvex lens is mounted in vacuum from the top flange. The lens focuses the LIF through a fused silica window out of the chamber onto a photomultiplier tube. For the VMII setup, a homemade ion optic (a repeller, extractor, and grounded lens) is inserted on the vertical axis, replacing the LIF lens. A 350 mm time-of-flight tube and a microchannel plate detector

coupled to a phosphor screen is added to the top of the vertical port. One of the hybrid turbo molecular pumps is removed from the scattering chamber and used to differentially pump the time-of-flight tube.

For the test system we chose nitric oxide (NO) for the molecule and Argon for the atom. NO is desirable due to its relative ease in detection; the same color photon can be used for both LIF detection and REMPI detection. In the REMPI scheme, when a second photon of the same color is absorbed by the NO molecule, the neutral molecule is ionized, and the ion is imaged using VMII. The transition we use is through the NO(A) state, which is near 226 nm. We use a Coherent Infinity laser with a 150mJ in a $\sim 6ns$ pulse at 1064 nm, which is tripled to produce 355 nm light. The 355 nm light then pumps a Lambda Physik SCANmate, running an Exiton Coumarin 450 dye. The output of the dye laser is doubled using a BBO-C crystal in an INRAD autotracker system to produce approximately 400 μJ of tunable radiation near 226 nm.

We operate the system with a 30 Hz repetition rate to compare with our traditional CAMB machine. At 30 Hz, with 1.05×10^5 Pa of stagnation pressure behind the valve, we observed a steady-state source pressure of $\sim 8\times10^{-4}$ Torr; a lower pressure than expected based on our calculations. The distance from the valve to the center of the ion optic is 13.9 cm. The steady-state background pressure in the main chamber is measured to be $\sim 7\times10^{-7}$ Torr, without baking. For the traditional CAMB machine, there is no pressure gauge on the source region, but there is a differential chamber between the source and the interaction region that is approximately 1×10^{-5} Torr, while the interaction region is 5×10^{-7} Torr.[16] The total distance between the valve and interaction region is 15 cm. Both apparatuses provide similar experimental conditions.

IV. RESULTS

We employed both LIF and VMII to characterize the effectiveness of the compact source chamber in producing a rotationally cold supersonic expansion with a narrow velocity spread. LIF was used to collect the rotationally resolved spectrum while VMII was used to record the molecular beam velocity, velocity spread, and NO–Ar scattering.

Figure 2 shows a typical LIF spectrum. The rotational distributions for the spectrum are assigned using the LIFBASE freeware.[17] The spectra do not fit to thermal distribution and so we do not rigourously assign a temperature. For comparisons with existing literature, we estimate the temperature based on the ratio of $J=1.5$ to $J=2.5$. All three valves, the PZT, EL, and General valve, were tested. The stagnation pressure for each valve was kept roughly constant with 1.05×10^5 Pa of 5% NO in an Ar carrier gas. The open time of each valve was varied to give the best expansion conditions for the given stagnation pressure while keeping the source pressure below 1×10^{-3} Torr at a 30 Hz repetition rate. Using the EL valve with a pulse length of approximately 35 μs, we obtained the LIF spectra shown in Fig. 2. The spectrum fits to an approximate rotational temperature of 5K. The PZT valve and General valve give similar performances for open times of 150 and 210 μs, respectively.

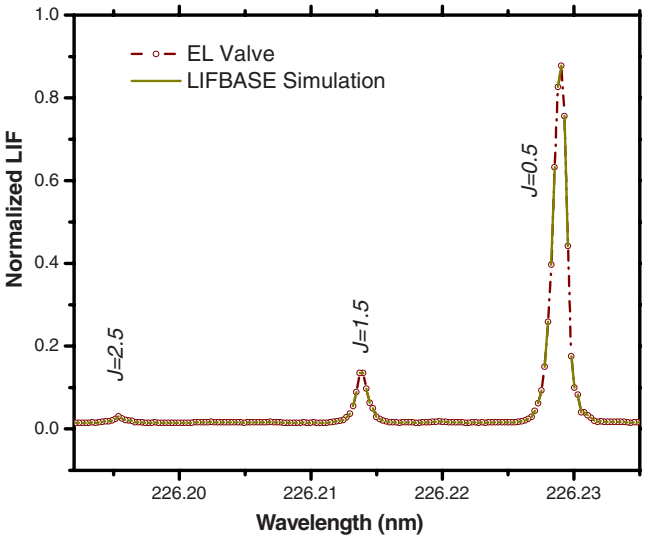

FIG. 2. (Color online) Spectrum of the NO(A) state taken using LIF imaging. The spectrum was simulated using LIFBASE freeware. The expansions do not fit to thermal distributions. The relative populations of $J=0.5$ to $J=3.5$ are adjusted for the best fit. The spectrum shown is for the EL valve with a 35 μs pulse and 1.05×10^5 Pa of stagnation pressure. The simulated spectrum has 83% in the $J=0.5$, 14% in the $J=1.5$, and 2% in the $J=2.5$ and nothing in the $J=3.5$ state.

The next major test of the apparatus was to operate it in a crossed-beam configuration, and attempt to observe scattering. For these experiments, the detection scheme is converted from LIF to VMII, and the apparatus is reconfigured as described in Sec. III.

Figure 3 shows a typical scattering ring for NO(X)$J=0.5$ scattering off of Ar to make NO(X)$J=7.5$ with 106.4 cm^{-1} of rotational energy transfer. The image was collected for 10 successive 30 s foreground and background images. For the foreground image, the timings of the AMB valves were adjusted such that the two beams temporally overlapped in the center of the scattering chamber, in order to maximize the scattering signal. For the background image, the atomic beam timing was shifted forward such that the atomic beam arrives in the scattering chamber 1 ms after the

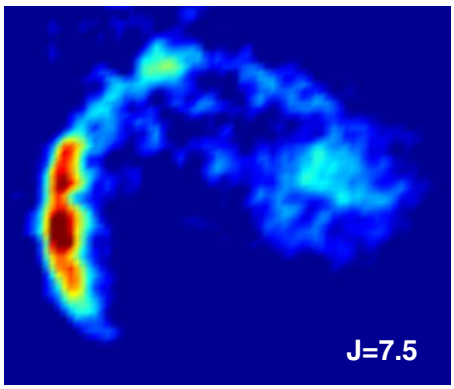

FIG. 3. (Color online) Image of NO$(X)_{j=7.5}$ formed by scattering NO$(X)_{j=0.5}$ off of a beam of neat Ar. The image obtained using VMII of NO$_{J=7.5}$ ionized by (1+1) REMPI through the NO(A) state. The pulses were produced using the PZT actuated valves with 150 μs pulses for both the 5% NO in Ar and the neat Ar beam. Both valves had a stagnation pressure of 1.05×10^5 Pa.

molecular beam. This effectively turns off the scattering with out affecting the steady state gas load in the chamber. The signal image is then constructed by subtracting the background images from the foreground images, and summing the differences.

The velocity of the molecular beam is directly measured by adding a 127.4 mm spacer between the source chamber and the scattering chamber. The spacer modifies the transit time of the molecules from the valve to the scattering region. From the length of the tube and the change in the transit time, we found the center velocity of the molecular beam to be 593.9 ± 4.7 m/s. From the VMII we identified the laboratory origin as the point where the molecular and atomic beams cross, by seeding the atomic beam with a trace amount of NO. Measuring the displacement of the molecular beam from the origin allows us to calibrate the ion-imaging detector. From this, we estimated the velocity spread of the molecular beam to be about 5%. This is nearly identical performance to what is observed in traditional molecular beam experiments.

V. CONCLUSION

We have constructed a compact molecular beam machine capable of both unimolecular and CAMB studies. The measured background pressures, scattering signals, and valve-to-interaction distances are all comparable to large CAMB machines. The entire C-CAMB apparatus, with our PZT valves and LIF imaging system cost less then 35K (USD) to assemble and operate; roughly the cost of one large turbo pump on our traditional CAMB machine. The C-CAMB machine has a footprint of 0.25 m^2 compared to the approximately 2.5 m^2 footprint of a traditional machine. We have successfully demonstrated the unimolecular beam operation by measuring the rotational temperatures achievable for several common valves. Further, we have demonstrated the CAMB operation by observing rotational energy transfer during collisions between $NO(X)j=0.5$ and Argon atoms.

Given the performance of this apparatus, we see no obvious disadvantages to the small size of the chambers for gas phase studies using ion imaging detection. If the experiment utilizes rotatable time-of-flight mass spectometers for energy analysis, the small size of the scattering chamber is not possible. As discussed in the introduction, these type of rotatable detectors necessitate large scattering chambers for angular resolution. However, the small size of the source chamber(s) still offers a clear financial advantage. Similarly, for experiments that scatter atomic and/or molecular beams off of surfaces; the small source design still offers clear advantages, while the small scattering chamber would not be ideal because of the space requirements for surface preparation and characterization. In general, the small compact source regions offer wide applicability to any experiment that utilizes pulsed atomic and/or molecular beams. The scattering chamber presented here must be tailored for the specific types of experiments one desires to explore.

Funding for this work was provided by the U. S. Department of Energy, Office of Basic Energy Science. Sandia National laboratory is a multidisciplinary laboratory operated by Sandia Corporation, a Lockheed Martin Co., for the United States Department of Energy.

[1] O. Stern, Zeitschrift fur Elektrochemie **25**, 66 (1919).
[2] O. Stern and W. Gerlach, Z. Phys. **9**, 353 (1922).
[3] I. I. Rabi and V. W. Cohen, Phys. Rev. **46**, 707 (1934).
[4] K. R. Wilson, G. H. Kwei, K. A. Norris, R. R. Herm, J. H. Birely, and D. R. Herschbach, J. Chem. Phys. **41**, 1154 (1964).
[5] D. R. Herschbach, Chem. Scr. **27**, 327 (1987).
[6] The Royal Swedish Academy of Sciences, Chemistry Nobel Prize press release, 1986.
[7] L. Zandee and R. B. Bernstein, J. Chem. Phys. **71**, 359 (1979).
[8] D. W. Chandler and P. L. Houston, J. Chem. Phys. **27**, 1445 (1987).
[9] A. G. Suits, L. S. Bontuyan, P. L. Houston, and B. J. Whitaker, J. Chem. Phys. **96**, 8618 (1992).
[10] *Atomic and Molecular Beam Methods*, edited by G. Scoles (Oxford University Press, New York, 1992), Vols. 1 and 2.
[11] *Atomic and Molecular Beams: State of the Art 2000*, edited by R. Campargue (Springer, New York, 2001).
[12] General Valve Corporation, Fairfield, NJ.
[13] D. Proch and T. Trickl, Rev. Sci. Instrum. **60**, 713 (1989).
[14] Jordan TOF Products, Inc., Grass Valley, CA.
[15] M. Hillenkamp, S. Keinan, and U. Even, J. Chem. Phys. **118**, 8699 (2003).
[16] T. K. Lorenz, M. S. Westley, and D. W. Chandler, Phys. Chem. Chem. Phys. **2**, 481 (2000).
[17] J. Luque, Database and Spectral simulation for diatomic molecules **2.0**.